Inorganic Chemistry

Article

Coordination Polymers Based on Cobridging of Rigid and Flexible Spacer Ligands: Syntheses, Crystal Structures, and Magnetic Properties of [Mn(bpy)(H$_2$O)(C$_4$H$_4$O$_4$)]·0.5bpy, Mn(bpy)(C$_5$H$_6$O$_4$), and Mn(bpy)(C$_6$H$_8$O$_4$)

Y.-Q. Zheng,* J.-L. Lin, and Z.-P. Kong

Municipal Key Laboratory of Solid State Chemistry & Materials Science, Institute for Solid State Chemistry, Ningbo University, Ningbo 315211, P. R. China

Reactions of 4,4′-bipyridine (bpy) with Mn(C$_4$H$_4$O$_4$)·4H$_2$O and Mn(C$_5$H$_6$O$_4$)·4H$_2$O in methanolic aqueous solutions yielded [Mn(bpy)(H$_2$O)(C$_4$H$_4$O$_4$)]·0.5bpy (**1**) and Mn(bpy)(C$_5$H$_6$O$_4$) (**2**), respectively, and reactions of freshly prepared Mn(OH)$_{2-2x}$(CO$_3$)$_x$·yH$_2$O, adipic acid and 4,4′-bipyridine in a methanolic aqueous solution afforded Mn(bpy)(C$_6$H$_8$O$_4$) (**3**). The six-coordinate Mn atoms in **1** are interlinked by flexible succinato ligands to form layers, which are sustained by rigid bpy ligands into an 3D open framework with the free bpy molecules in tunnels. The ribbonlike chains in **2** result from Mn atoms bridged by glutarato ligands and are connected by bpy ligands into open layers. In **3**, the Mn atoms are bridged by both bpy and adipato ligands to form 3D nanoporous frameworks and 2-fold interpenetration of the resulting 3D frameworks completes the crystal structure. In comparison with **1** and **2**, compound **3** displays significant antiferromagnetic behavior at low temperature. The antiferromagnetic exchange becomes stronger from **1** through **2** to **3**, and the antiferromagnetic ordering of Mn^{2+} centers is related to the syn–syn bridging mode of the terminal carboxylate groups of α,ω-dicarboxylate anions. Crystal data: C$_{19}$H$_{18}$MnN$_3$O$_5$ (**1**), monoclinic *P*2$_1$/*c*, *a* = 11.686(2) Å, *b* = 17.847(2) Å, *c* = 8.852(1) Å, *β* = 99.67(1)°, *V* = 1819.9(4) Å^3, *Z* = 4, *D$_c$* = 1.545 g·cm^{-3}; C$_{15}$H$_{14}$MnN$_2$O$_4$ (**2**), triclinic *P*$\bar{1}$, *a* = 8.145(2) Å, *b* = 9.574(2) Å, *c* = 10.180(1) Å, α = 108.01(3)°, *β* = 93.55(3)°, γ = 105.30(1)°, *V* = 719.2(2) Å^3, *Z* = 2, *D$_c$* = 1.576 g·cm^{-3}; C$_{15}$H$_{14}$MnN$_2$O$_4$ (**3**), triclinic *P*$\bar{1}$, *a* = 8.544(1) Å, *b* = 8.881(1) Å, *c* = 10.949(2) Å, α = 108.81(1)°, *β* = 95.40(1)°, γ = 101.94(1)°, *V* = 757.7(2) Å^3, *Z* = 2, *D$_c$* = 1.557 g·cm^{-3}.

Introduction

The rational design and synthesis of metal−organic frameworks (MOFs) with specific topologies have been the most important subjects of intensive current research in coordination chemistry, supramolecular chemistry and materials science.[1] Since long, neutral rigid N-donor ligands such as 4,4′-bipyridine have been widely used to construct supramolecular architectures, thus formed metal−organic frameworks are charge-compensated by counterionic guests in the cavities of the solid and removal of the guests normally leads to damage of the frameworks. Utilization of rigid aromatic dicarboxylate ligands has become an interesting strategy to construct neutral nanoporous coordination polymers.[2−4] Different from the rigid dicarboxylate spacer ligands, the saturated aliphatic dicarboxylate ligands exhibit conformational and coordination versatility due to single-bonded carbon chains and are viewed as important flexible spacer ligands. Under mild ambient and hydrothermal

(1) (a) Evans, O. R.; Lin, W. *Acc. Chem. Res.* **2002**, *35*, 511. (b) Moulton, B.; Zaworotko, M. J. *Chem. Rev.* **2001**, *101*, 1629. (c) Swiegers, G. F.; Malefeste, T. J. *Chem. Rev.* **2000**, *100*, 3483. (d) Kaes, C.; Katz, A.; Hosseini, M. W. *Chem. Rev.* **2000**, *100*, 3553. (e) Carlucci, L.; Ciani, G.; Moret, M.; Proserpio, D. M.; Rizzato, S. *Angew. Chem., Int. Ed.* **2000**, *39*, 1506. (f) Zaworotko, M. J. *Angew. Chem., Int. Ed.* **2000**, *39*, 3052. (g) Batten, S. R.; Robson, R. *Angew. Chem., Int. Ed.* **2000**, *37*, 1460. (h) Hagrman, P. J.; Hagrman, D.; Zubieta, J. *Angew. Chem., Int. Ed.* **1999**, *38*, 2638.

(2) Li, H.; Eddaoudi, M.; O'Keeffe, M.; Yaghi, O. M. *Nature* **1999**, *402*, 276.

(3) Chui, S. S.-Y.; Lo, S. M.-F.; Charmant, J. P. H.; Orpen, A. G.; William, I. D. *Science* **1999**, *283*, 1148.

(4) Serre, C.; Millange, F.; Thouvenot, C.; Noguès, M.; Marsolier, G.; Louër, D.; Férey, G. *J. Am. Chem. Soc.* **2002**, *124*, 13519.

conditions, self-assembly of metal cations with α,ω-dicarboxylate anions afforded a variety of supramolecular motifs, where the discrete metal—oxygen polyhedra could be interconnected by organic linkers into polymeric chains, layers and 3D frameworks, and unfortunately, such 3D frameworks exhibit normally little porosity.[5−15] To overcome this problem, our recent research has been intensively focused on simultaneous utilization of rigid N-donor ligands and α,ω-dicarboxylate ligands to construct coordination polymers. Hitherto, however, reports about simultaneous bridging of rigid 4,4′-bipyridine and flexible α,ω-dicarboxylate ligands to construct coordination polymers are very scarce,[16] and the first reported example was a copper(II) malonato complex with 4,4′-bipyridine, $[Cu_2(C_3H_2O_4)_2(H_2O)_2(bpy)]\cdot H_2O$, in which the flexible malonato and rigid 4,4′-bipyridine ligands are combined to coordinate Cu atoms into two-dimensional square networks.[17] Our recent investigation on self-assembly of Cu(II) cations, 4,4′-bipyridine and succinate anions in a methanolic aqueous solution under ambient conditions produced a new porous coordination polymers resulting from the helical Cu succinato chains interconnected with 4,4′-bipyridine ligands.[18] Here, we report three Mn(II) coordination polymers, $[Mn(bpy)(H_2O)(C_4H_4O_4)]\cdot 0.5bpy$ (**1**), Mn-(bpy)($C_5H_6O_4$) (**2**) and Mn(bpy)($C_6H_8O_4$) (**3**), where the Mn atoms are bridged by flexible succinato, glutarato and adipato ligands to generate 2D layers, 1D ribbonlike chains and 2D square gridlike layers, respectively, and they are pillared by rigid bpy ligands into higher dimensional frameworks.

Experimental Section

Except $Mn(C_4H_4O_4)\cdot 4H_2O^{6h}$ and $Mn(C_5H_6O_4)\cdot 4H_2O,^{6d}$ which were prepared in our laboratory, all chemicals of reagent grade were commercially available and used without further purification. The C, N and H microanalyses were performed with a Heraeus Rapid-CHNO elemental analyzer. The FT-IR spectra were recorded from KBr pellets in the range $4000-400$ cm^{-1} on a Shimadzu FTIR-8900 spectrometer. The magnetic susceptibilities were measured using a SQUID magnetometer (Quantum Design model MPMS-7) in temperature range $5 \leq T$ (K) ≤ 300 with an applied field of 10 000 G. Diamagnetic corrections were estimated from Pascal's constants.[19] Thermogravimetric measurements were carried out from room temperature to 600 °C on preweighed samples in a nitrogen stream using a Seiko Exstar6000 TG/DTA6300 apparatus with a heating rate of 10 °C/min.

Synthesis of $[Mn(bpy)(H_2O)(C_4H_4O_4)]\cdot 0.5bpy$ (1). A methanolic solution of 0.100 g (0.52 mmol) of 4,4′-bipyridine dihydrate in 5.0 mL of CH_3OH was dropwise added to a stirred aqueous solution of 0.127 g (0.52 mmol) of $Mn(C_4H_4O_4)\cdot 4H_2O$ in 20 mL of H_2O to produce a nearly colorless solution (pH = 7.05). Yellow needlelike crystals were grown by slow evaporation at room temperature for 1 month. Yield: ca. 75% based on the initial Mn-$(C_4H_4O_4)\cdot 4H_2O$ input. Anal. Calcd for $C_{19}H_{18}MnN_3O_5$: C, 53.91; H, 4.29; N, 9.93. Found: C, 53.74; H, 4.37; N, 10.08. IR (cm^{-1}): 3329 m (broad), 1624 (shoulder), 1556 vs, 1541 vs, 1404 s, 1387 s, 1220 w, 1153 w, 1061 w, 819 m, 802 m, 736 w, 663 m, 646 m, 621 w. When heated in a flowing nitrogen atmosphere, compound **1** releases 1 H_2O and 1.5 bpy molecules over $150-338$ °C with the weight loss of 60.0% corresponding well to the calculated value of 59.60%. Over $340-490$ °C, the investigated sample loses additional weight of 23.8%, suggesting sublimation of one succinic anhydride (calculated value: 23.64%) with the residue identified to be MnO.

Synthesis of Mn(bpy)($C_5H_6O_4$) (2). 2 was prepared analogously to **1** except that 0.106 g (0.52 mmol) of $Mn(C_5H_6O_4)\cdot 4H_2O$ was used in place of $Mn(C_4H_4O_4)\cdot 4H_2O$. The resulting solution (pH = 6.71) was kept at 50 °C, and slow evaporation for about 2 months afforded yellow needlelike crystals. Yield: ca. 84% based on the initial $Mn(C_5H_6O_4)\cdot 4H_2O$ input. Anal. Calcd for $C_{15}H_{14}MnN_2O_4$: C, 52.80; H, 4.14; N, 8.21. Found: C, 52.94; H, 4.27; N, 8.33. IR (cm^{-1}): 3085 w, 3061 w, 3045 w, 2953 w, 2907 w, 1602 vs, 1587 vs, 1556 vs, 1489 m, 1454 s, 1410 vs, 1340 m, 1319 m, 1306 m, 1237 w, 1290 vw, 1219 m, 1156 w, 1065 m, 1040 m, 1005 m, 909 w, 826 m, 814 vs, 719 m, 629 vs, 479 w. The TGA shows that **2** is stable below 240 °C. The weight loss of 78.5% over $240-503$ °C suggests liberation of one bpy and one glutaric anhydride molecules (calculated value: 79.21%), and the white residue of 21.5% collected at 600 °C is very close to the calculated value of 20.79% expected for MnO solid.

Synthesis of Mn(bpy)($C_6H_8O_4$) (3). A 1.0 mL (1 M) volume of Na_2CO_3 was dropwise added to an aqueous solution of 0.088 g (0.5 mmol) of $MnSO_4\cdot H_2O$ in 5.0 mL of H_2O to yield yellow precipitate, which was centrifuged and washed with water until no SO_4^{2-} anions were detectable. The collected precipitate was then

(5) (a) Gupta, M. P.; Devi, B. P. *Curr. Sci.* **1978**, *47*, 336. (b) Sharrock, P.; Theophanides, T. *Can. J. Chem.* **1975**, *53*, 98. (c) Suresh, E.; Bhadbhade, M. M.; Venkatasubramanian, K. *Polyhedron* **1999**, *18*, 657. (d) O'Connor, B. H.; Maslen, E. N. *Acta Crystallogr.* **1966**, *20*, 824.

(6) (a) Zheng, Y.-Q.; Lin, J.-L. *Z. Kristallogr.—New Cryst. Struct.* **2000**, *215*, 157. (b) Zheng, Y.-Q.; Lin, J.-L. *Z. Kristallogr.—New Cryst. Struct.* **2000**, *215*, 159. (c) Zheng, Y.-Q.; Pan, A.-Y.; Lin, J.-L. *Z. Kristallogr.—New Cryst. Struct.* **2000**, *215*, 263. (d) Zheng, Y.-Q.; Lin, J.-L.; Sun, J.; Zhang, H.-L. *Z. Kristallogr.—New Cryst. Struct.* **2000**, *215*, 163. (e) Zheng, Y.-Q.; Zhou, S.-Q.; Lin, J.-L. *Z. Kristallogr.—New Cryst. Struct.* **2001**, *216*, 265. (f) Zheng, Y.-Q.; Lin, J.-L.; Chen, W.-J. *Z. Kristallogr.—New Cryst. Struct.* **2001**, *216*, 269. (g) Zheng, Y.-Q.; Lin, J.-L. *Z. Kristallogr.—New Cryst. Struct.* **2000**, *215*, 165. (h) Zheng, Y.-Q.; Sun, J.; Lin, J.-L. *Z. Kristallogr.—New Cryst. Struct.* **2002**, *217*, 411.

(7) (a) Fleck, M.; Tillmanns, E.; Bohaty, L. *Z. Kristallogr.—New Cryst. Struct.* **2000**, *215*, 619. (b) Rastsvetaeva, R. K.; Pushcharovsky, D. Yu.; Furmanova, N. G. *Z. Kristallogr.* **1996**, *211*, 808.

(8) (a) Zheng, Y.-Q.; Lin, J.-L.; Pan, A.-Y. *Z. Anorg. Allg. Chem.* **2000**, *626*, 1718. (b) Zheng, Y.-Q.; Lin, J.-L.; Sun, J.; Pan, A.-Y. *Z. Kristallogr.—New Cryst. Struct.* **2000**, *215*, 161.

(9) (a) Zheng, Y.-Q.; Karl, P.; von Schnering, H. G. *Chem. Res. Chin. Univ.* **2001**, *17*, 20. (b) Zheng, Y.-Q.; Lin, J.-L.; Zhang, H.-L. *Z. Kristallogr.—New Cryst. Struct.* **2000**, *215*, 535. (c) Zheng, Y.-Q.; Pan, A.-Y.; Lin, J.-L. *Z. Kristallogr.—New Cryst. Struct.* **2001**, *216*, 267. (d) Michaelides, A.; Kiritsis, V.; Skoulika, S.; Aubry, A. *Angew. Chem., Int. Ed. Engl.* **1993**, *32*, 1495.

(10) (a) Zheng, Y.-Q.; Kong, Z.-P. *J. Solid State Chem.* **2002**, *166*, 279. (b) Kim, Y. J.; Lee, E. W.; Jung, D.-Y. *Chem. Mater.* **2001**, *13*, 2684. (c) Kim, Y. J.; Jung, D.-Y. *Inorg. Chem.* **2000**, *39*, 1470. (d) Kim, Y. J.; Jung, D.-Y. *Bull. Korean Chem. Soc.* **2000**, *21*, 656.

(11) (a) Livage, C.; Egger, C.; Férey, G. *J. Mater. Chem.* **1998**, *8*, 2743. (b) Livage, C.; Egger, C.; Férey, G. *Chem. Mater.* **1999**, *11*, 1546. (c) Kim, Y. J.; Jung, D.-Y. *Bull. Korean Chem. Soc.* **1999**, *20*, 827.

(12) Forster, P. M.; Cheetham, A. K. *Angew. Chem., Int. Ed.* **2002**, *41*, 457.

(13) Livage, C.; Egger, C.; Férey, G. *Chem. Mater.* **2001**, *13*, 410.

(14) Zheng, Y.-Q.; Lin, J.-L. *Z. Kristallogr.—New Cryst. Struct.* **2001**, *216*, 139.

(15) (a) Lee, E. W.; Kim, Y. J.; Jung, D.-Y. *Inorg. Chem.* **2002**, *41*, 501. (b) Livage, C.; Egger, C.; Férey, G. *C. R. Acd. Sci., Ser. IIc: Chim.* **2001**, *4*, 221.

(16) Li, J. M.; Zhang, Y. G.; Chen, J. H.; Rui, L.; Wang, Q. M.; Wu, X. T. *Polyhedron* **2000**, *19*, 1117.

(17) Li, J. M.; Zeng, H.; Chen, J.; Wang, Q.; Wu, X. *Chem. Commun.* **1997**, 1213.

(18) Zheng, Y.-Q.; Kong, Z.-P. *Z. Anorg. Allg. Chem.* **2003**, *629*, 1469.

(19) Boudreaux, E. A.; Mulay, L. N. *Theory and Applications of Molecular Paramagnetism*; John Wiley & Sons: New York, 1976.

Table 1. Crystal Data and Structure Refinement Parameters for Compounds **1**−**3**

param	1	2	3
empirical formula	$C_{19}H_{18}MnN_3O_5$	$C_{15}H_{14}MnN_2O_4$	$C_{16}H_{16}MnN_2O_4$
formula mass	423.30	341.22	355.25
cryst system	monoclinic	triclinic	triclinic
space group	$P2_1/c$	$P\bar{1}$	$P\bar{1}$
a (Å)	11.686(2)	8.145(2)	8.544(1)
b (Å)	17.847(2)	9.574(2)	8.881(1)
c (Å)	8.852(1)	10.180(2)	10.949(2)
α (deg)		108.01(3)	108.81(1)
β (deg)	99.67(1)	93.55(3)	95.40(1)
γ (deg)		105.30(3)	101.94(1)
V (Å³)	1819.9(4)	719.2(2)	757.7(2)
Z	4	2	2
D_{calc} (g cm⁻³)	1.545	1.576	1.557
$F(000)$	872	350	366
μ (mm⁻¹)	0.763	0.937	0.893
θ range (deg)	1.77−27.50	2.13−27.50	2.00−27.49
tot. no. of data collcd	4175	3953	4084
no. of obsd data ($I \geq 2\sigma(I)$)	2464	3260	3401
R_1, wR_2 [$I \geq 2\sigma(I)$][a]	0.0545, 0.0983	0.0364, 0.0883	0.0512, 0.1220
R_1, wR_2 (all data)[a]	0.1193, 0.1196	0.0492, 0.0945	0.0663, 0.1281
goodness-of-fit on F^2	1.010	1.053	1.175
no. of variables	265	201	214
largest diff peak and hole (e Å⁻³)	0.423, −0.518	0.469, −0.313	0.435, −0.400

[a] $R_1 = \sum(|F_o| - |F_c|)/\sum|F_o|$, $wR_2 = [\sum w(F_o^2 - F_c^2)^2/\sum w(F_o^2)^2]^{1/2}$, and $w = [\sigma^2(F_o^2) + (aP)^2 + bP]^{-1}$, where $P = (F_o^2 + 2F_c^2)/3$. For **1**, $a = 0.0436$ and $b = 0.2776$. For **2**, $a = 0.0415$ and $b = 0.2308$. For **3**, $a = 0.0235$ and $b = 1.4420$.

added to a stirred aqueous solution of 0.076 g (0.52 mmol) of adipic acid in 20 mL of H_2O to give a brown suspension, to which was added a methanolic solution of 0.100 g (0.52 mmol) of 4,4′-bipyridine dihydrate in 5.0 mL of CH_3OH. The mixture was further stirred for another 30 min. The insoluble solid was filtered out, and the filtrate (pH = 5.89) was allowed to stand at room temperature. On the next day, tiny yellow crystals grew. Yield: ca. 37% based on the initial $MnSO_4{\cdot}H_2O$ input. Anal. Calcd for $C_{16}H_{16}MnN_2O_4$: C, 54.10; H, 4.54; N, 7.89. Found: C, 54.07; H, 4.76; N, 7.61. IR (cm⁻¹): 3064 w, 3042 w, 2953 s, 2909 w, 2856 w, 1591 vs, 1551 vs, 1487 s, 1431 vs, 1335 m, 1296 s, 1236 vw, 1217 s, 1140 m, 1063 s, 1042 m, 1003 m, 914 w, 816 vs, 802 s, 757 w, 731 m, 626 vs, 507 vw, 476 vw, 466 vw. The thermogravimetric analyses indicate that **3** starts decomposition at 237 °C and the weight loss of 79.1% over 237−380 °C is slightly less than the value of 80.03% expected for sublimation of one bpy and one adipic anhydride molecules per formula unit. The white residue of 19.5% collected at 600 °C is identified to be MnO according to powder X-ray diffraction patterns.

X-ray Crystallography. Suitable single crystals were selected under a polarizing microscope and fixed with epoxy cement on respective fine glass fibers which were then mounted on a Bruker P4 diffractomerter with graphite-monochromated Mo Kα radiation (λ = 0.710 73 Å) for cell determination and subsequent data collection. The lattice parameters were refined from the 2ϑ values (10−25°) of 25 carefully centered reflections. The reflection intensities with $2\vartheta_{max}$ = 55° were collected at 293 K using the ϑ−2ϑ scan technique. The data were corrected for Lp and absorption effects. SHELXS-97 and SHELXL-97 programs[20,21] were used for structure solution and refinement. The structures were solved by using direct methods. Subsequent difference Fourier syntheses enabled all non-hydrogen atoms to be located. All hydrogen atoms associated with carbon atoms were geometrically generated except that those bonded to the C(15) and two split carbon atoms C(16a) and C(16b) of the distorted adipate anion in **3** were not located. The aqua hydrogen atoms of **1** were located from the successive difference Fourier syntheses. Finally, all non-hydrogen

(20) Sheldrick, G. M. *SHELXS-97, Program for Crystal Structure Solution*; University of Göttingen: Göttingen, Germany, 1997.
(21) Sheldrick, G. M. *SHELXL-97, Program for Crystal Structure Refinement*; University of Göttingen: Göttingen, Germany, 1997.

Table 2. Selected Interatomic Distances (Å) and Bond Angles (deg) for **1**[a]

Mn−O(1)	2.161(2)	Mn−O(4)#2	2.140(2)	Mn−N(1)	2.295(3)
Mn−O(3)#5	2.190(2)	Mn−O(5)	2.172(3)	Mn−N(2)#4	2.296(3)

O(1)−Mn−O(3)#5	176.6(1)	O(3)#5−Mn−N(2)#4	87.3(1)
O(1)−Mn−O(4)#2	96.2(1)	O(4)#2−Mn−O(5)	177.3(1)
O(1)−Mn−O(5)	84.4(1)	O(4)#2−Mn−N(1)	88.3(1)
O(1)−Mn−N(1)	91.4(1)	O(4)#2−Mn−N(2)#4	89.8(1)
O(1)−Mn−N(2)#4	89.3(1)	O(5)−Mn−N(1)	89.1(1)
O(3)#5−Mn−O(4)#2	83.2(1)	O(5)−Mn−N(2)#4	92.8(1)
O(3)#5−Mn−O(5)	96.4(1)	N(1)−Mn−N(2)#4	178.0(1)
O(3)#5−Mn−N(1)	91.9(1)		

[a] Symmetry transformations used to generate equivalent atoms: #1 = x + 1, y, z; #2 = $-x$ + 1, $-y$ + 2, $-z$; #3 = $-x$ + 1, y + 1/2, $-z$ + 1/2; #4 = x − 1, y, z; #5 = $-x$ + 1, y − 1/2, $-z$ + 1/2; #6 = $-x$ + 2, $-y$ + 2, $-z$.

atoms were refined with anisotropic displacement parameters by the full-matrix least-squares technique and hydrogen atoms were refined with isotropic displacement parameters. Detailed information about the crystal data and structure determination is summarized in Table 1. Selected interatomic distances and bond angles are given in Tables 2−4. Crystallographic data (excluding structure factors) for the structures in this paper have been deposited with Cambridge Crystallographic Data Centre as supplementary publication nos. CCDC 231937 ($C_{19}H_{18}MnN_3O_5$), CCDC 231938 ($C_{15}H_{14}MnN_2O_4$), and CCDC 231939 ($C_{15}H_{14}MnN_2O_4$). Copies of the data can be obtained, free of charge, on application to CCDC, 12 Union Road, Cambridge CB2 1EZ, U.K. (fax +44 1223 336033 or e-mail deposit@ccdc.cam.ac.uk).

Results and Discussion

Description of the Crystal Structures

[Mn(bpy)(H₂O)(C₄H₄O₄)]·0.5bpy (1). The asymmetric unit contains one Mn^{2+} cation, one succinate anion, one H_2O molecule, and one and a half 4,4′-bipyridine molecules. As depicted in Figure 1, the Mn atoms are each octahedrally coordinated by two N atoms of different bpy ligands and four O atoms of one H_2O molecule and three succinato groups with the N atoms at the trans positions. The Mn−O bond distances fall in the region 2.140−2.190 Å, and both
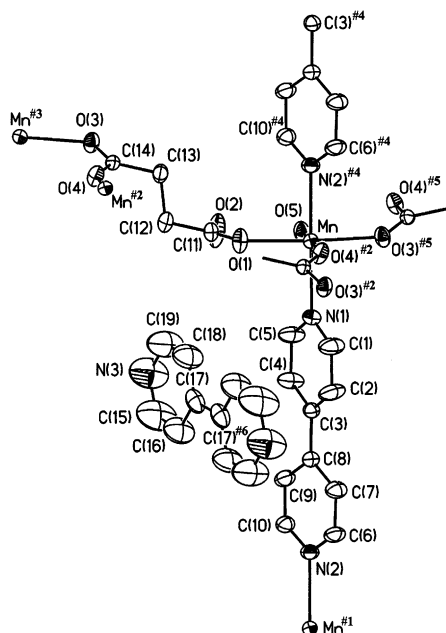
Figure 1. ORTEP view of coordination environments of Mn atoms along with the bridging types of succinato and 4,4′-bipyridine ligands and the atomic labeling for **1**. The displacement ellipsoids are drawn at 60% probability level (Symmetry transformations used to generate equivalent atoms: #1 = $x + 1, y, z$; #2 = $-x + 1, -y + 2, -z$; #3 = $-x + 1, y + 1/2, -z + 1/2$; #4 = $x - 1, y, z$; #5 = $-x + 1, y - 1/2, -z + 1/2$; #6 = $-x + 2, -y + 2, -z$).

Mn−N bond distances averaging 2.296 Å are practically identical within the experimental limitation (Table 2). The cisoid and transoid bond angles about the central Mn atom are in the regions 83.2−96.2 and 176.6−178.0°, respectively, exhibiting slight deviation from the corresponding ideal values of a regular octahedron. Two carboxylate groups of the *anti* succinato ligand have two coordination modes. In the first mode, the carboxylate group bidentately bridges two Mn atoms in *syn−anti* fashion and the other monatomically coordinates one Mn atom in the *syn* fashion. The Mn atoms are interlinked by the succinato ligands to generate 2D layers parallel to (100). The resulting layer is composed practically of 14- and 22-membered rings (Figure 2). The aqua ligand in the larger ring donates the hydrogen atoms to the uncoordinating carboxylate O(2) atom and the *syn*-coordinating carboxylate O(3) ($-x + 1, -y + 2, -z + 1$) to form two intralayer hydrogen bonds with $d(\text{O}\cdots\text{O}) = 2.600$ and 2.802 Å. The Mn$\cdots$Mn separation over the bridging carboxylate group is 5.264(1) Å, and the shortest distance due to the succinato group is 7.381(1) Å. The resulting layers are strutted by the rigid 4,4′-bipyridine ligands to form a 3D open framework exhibiting two kinds of tunnels, which propagate infinitely along the [001] and [101] directions, respectively. The Mn$\cdots$Mn distance due to 4,4′-bipyridine ligand is 11.686(2) Å. The neighboring 4,4′-bipyridine ligands orientate nearly perpendicularly to one another with the side C−H bonds directed to the pyridyl plane of the adjacent bpy ligand. The H-to-plane distances in the region are 2.95−3.18 Å, indicating weak C−H$\cdots\pi$ interactions.[22] The formed 3D framework is obviously stabilized by the free 4,4′-bipyridine molecules, which reside at the crossing positions of the tunnels (Figure 2). Different from the
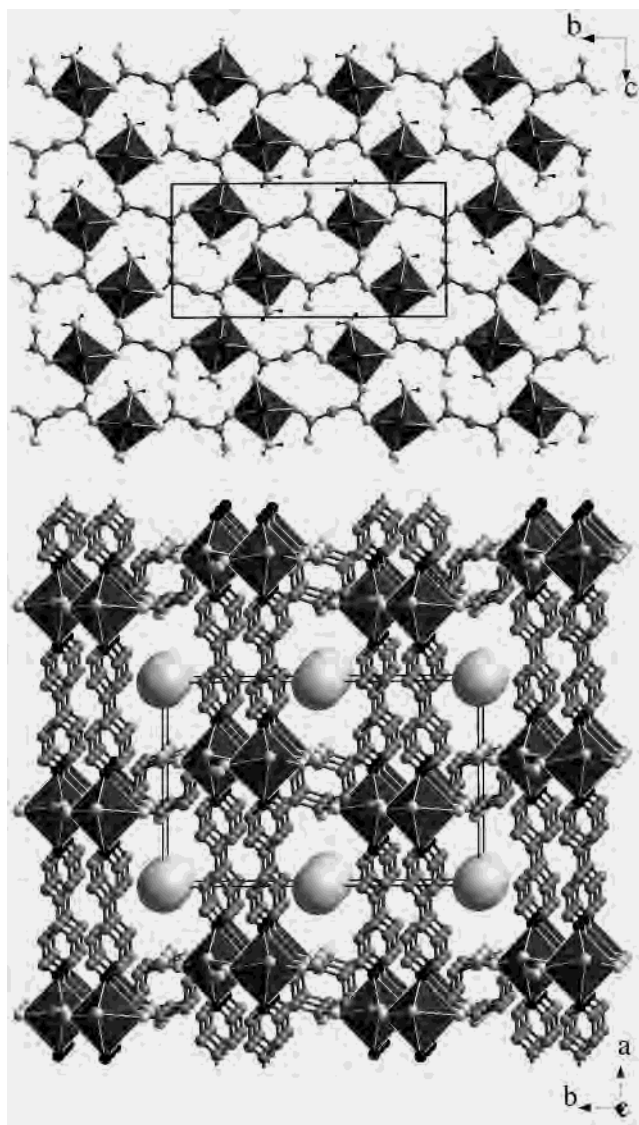
Figure 2. Top: 2D layer of six-coordinate Mn atoms bridged by succinato ligands in **1**. Bottom: Crystal structure of **1** (the larger gray balls representing free bpy molecules).

coplanar 4,4′-bipyridine molecule, the bpy ligand is twisted with the dihedral angle of 9.1(3)° between two pyridyl components.

Mn(bpy)(C₅H₆O₄) (2). The asymmetric unit of **2** contains one Mn²⁺ cation, one bpy ligand, and one (C₅H₆O₄)²⁻ glutarate anion. As shown in Figure 3, the Mn atoms are each in a severely distorted octahedral coordination sphere defined by two N atoms of two bpy ligands and four O atoms of three glutarate anions with $d(\text{Mn}-\text{N}) = 2.267$ and 2.271 Å and $d(\text{Mn}-\text{O}) = 2.103-2.374$ Å (Table 3). The terminal carboxylate groups of each gauche glutarate anion display different coordination modes, one bidentately bridging two Mn atoms in *syn−syn* fashion and the other chelating one Mn atom. Along the [100] direction, the octahedra are bridged by the glutarate anions to generate ribbonlike chains containing 8- and 16-membered rings (Figure 4). Within the

(22) Janiak, C.; Temizdemir, S.; Dechert, S.; Deck, W.; Girgsdies, F.; Heinze, J.; Kolm, M. J.; Scharmann, T. G.; Zipffel, O. M. *Eur. J. Inorg. Chem.* **2000**, 1229.

Table 3. Selected Interatomic Distances (Å) and Bond Angles (deg) for **2**[a]

Mn−O(1)#3	2.103(2)	C(11)−O(2)	1.245(3)
Mn−O(2)	2.137(2)	C(11)−C(12)	1.503(3)
Mn−O(3)#5	2.194(2)	C(12)−C(13)	1.509(4)
Mn−O(4)#5	2.374(2)	C(13)−C(14)	1.513(4)
Mn−N(1)	2.267(2)	C(14)−C(15)	1.507(4)
Mn−N(2)#4	2.271(2)	C(15)−P(3)	1.239(3)
C(11)−O(1)	1.244(3)	C(15)−O(4)	1.239(4)

|			
O(1)#3−Mn−O(2)	125.04(9)	O(3)#5−Mn−O(4)#5	56.36(7)
O(1)#3−Mn−O(3)#5	92.26(9)	O(3)#5−Mn−N(1)	93.87(8)
O(1)#3−Mn−O(4)#5	147.88(9)	O(3)#5−Mn−N(2)#4	89.58(8)
O(1)#3−Mn−N(1)	89.29(7)	O(4)#5−Mn−N(1)	86.52(7)
O(1)#3−Mn−N(2)#4	86.45(7)	O(4)#5−Mn−N(2)#4	98.84(7)
O(2)−Mn−O(3)#5	142.27(8)	N(1)−Mn−N(2)#4	174.62(7)
O(2)−Mn−O(4)#5	86.96(7)	O(1)−C(11)−O(2)	125.0(2)
O(2)−Mn−N(1)	92.21(8)	O(3)−C(15)−O(4)	120.4(2)
O(2)−Mn−N(2)#4	87.57(8)		

[a] Symmetry transformations used to generate equivalent atoms: #1 = $x, y - 1, z - 1$; #2 = $x - 1, y, z$; #3 = $-x + 1, -y + 2, -z + 1$; #4 = $x, y + 1, z + 1$; #5 = $x + 1, y, z$.
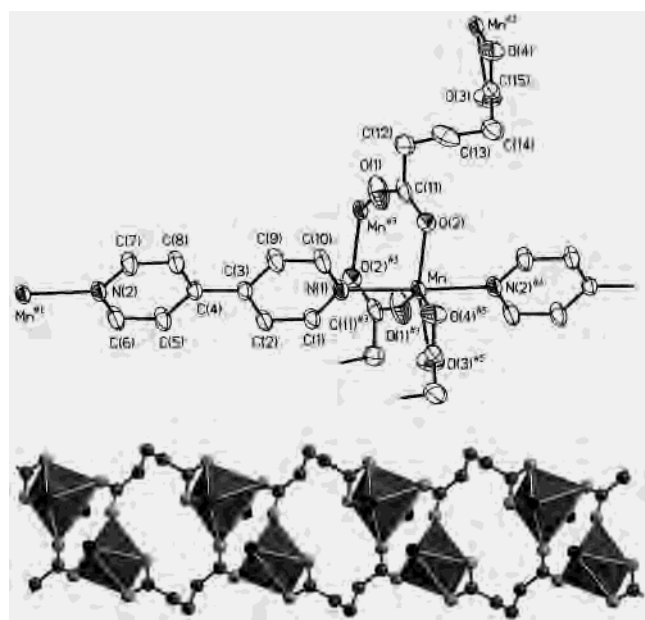
Figure 3. Top: ORTEP view of coordination environments of Mn atoms along with bridging fashions of glutarato and 4,4′-bipyridine ligands and the atomic labeling for **2**. The displacement ellipsoids are drawn at 60% probability level (Symmetry transformations used to generate equivalent atoms: #1 = $x, y - 1, z - 1$; #2 = $x - 1, y, z$; #3 = $-x + 1, -y + 2, -z + 1$; #4 = $x, y + 1, z + 1$; #5 = $x + 1, y, z$). Bottom: 1D ribbonlike chains of Mn atoms bridged by glutarato ligands.

8-membered ring, the Mn···Mn separation is 3.973(1) Å. The closest Mn···Mn distance within the 16-membered ring is 6.486(2) Å. The resulting chains are interlinked by the bidentate bpy ligands into gridlike layers containing rhombic apertures, and the Mn···Mn distance due to 4,4′-bipyridine ligand is 11.620(5) Å. Parallel to (01$\bar{1}$), the 2D layers are close-packed so that each layer is shifted by $(\vec{b} + \vec{c})/2$ with respect to the next one (Figure 4).

Mn(bpy)(C₆H₈O₄) (3). The symmetric unit comprises one Mn²⁺ cation, one bpy molecule and two adipate anions, of which one is disordered. Similar to **2**, the Mn atoms are each coordinated by two pyridyl N atoms at the trans positions and four O atoms from one chelating and two μ_2 bridging-carboxylate groups to complete significantly distorted octahedra (Figure 5). The Mn−O bond distances fall in the
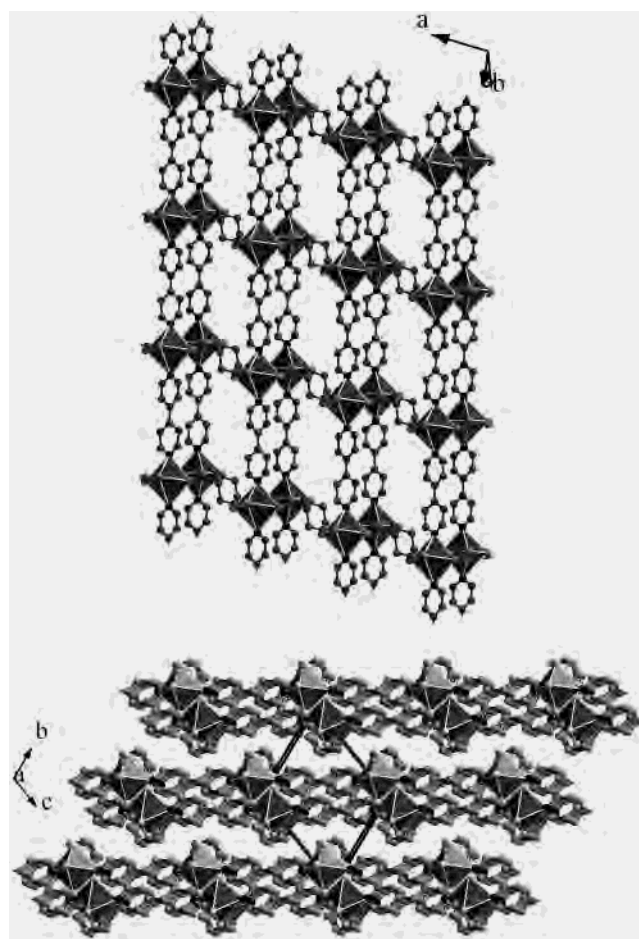

Figure 4. Top: Ribbonlike chains pillared by rigid bpy ligands into a 2D layer. Bottom: Crystal structure of **2**.

Table 4. Selected Interatomic Distances (Å) and Bond Angles (deg) for **3**[a]

Mn−O(1)	2.097(3)	C(11)−O(1)	1.241(4)	C(14)−O(4)	1.251(5)
Mn−O(2)#2	2.088(3)	C(11)−O(2)	1.243(4)	C(14)−C(15)	1.499(6)
Mn−O(3)	2.261(3)	C(11)−C(12)	1.503(5)	C(15)−C(16A)	1.473(9)
Mn−O(4)	2.254(3)	C(12)−C(13)	1.508(5)	C(15)−C(16B)	1.535(9)
Mn−N(1)	2.280(3)	C(13)−C(13)#4	1.533(7)	C(16A)−C(16B)#5	1.552(12)
Mn−N(2)#3	2.295(3)	C(14)−O(3)	1.256(5)		

O(1)−Mn−O(2)#2	120.0(1)	O(3)−Mn−O(4)	57.6(1)
O(1)−Mn−O(3)	149.4(1)	O(3)−Mn−N(1)	92.3(1)
O(1)−Mn−O(4)	92.1(1)	O(3)−Mn−N(2)#3	88.0(1)
O(1)−Mn−N(1)	91.9(1)	O(4)−Mn−N(1)	91.3(1)
O(1)−Mn−N(2)#3	87.5(1)	O(4)−Mn−N(2)#3	88.2(1)
O(2)#2−Mn−O(3)	90.0(1)	N(1)−Mn−N(2)#3	179.3(1)
O(2)#2−Mn−O(4)	147.4(1)	O(1)−C(11)−O(2)	125.6(3)
O(2)#2−Mn−N(1)	93.2(1)	O(3)−C(14)−O(4)	120.3(4)
O(2)#2−Mn−N(2)#3	87.5(1)		

[a] Symmetry transformations used to generate equivalent atoms: #1 = $x, y - 1, z - 1$; #2 = $-x + 1, -y + 2, -z + 1$; #3 = $x, y + 1, z + 1$; #4 = $-x + 2, -y + 3, -z + 1$; #5 = $-x + 2, -y + 2, -z + 2$.
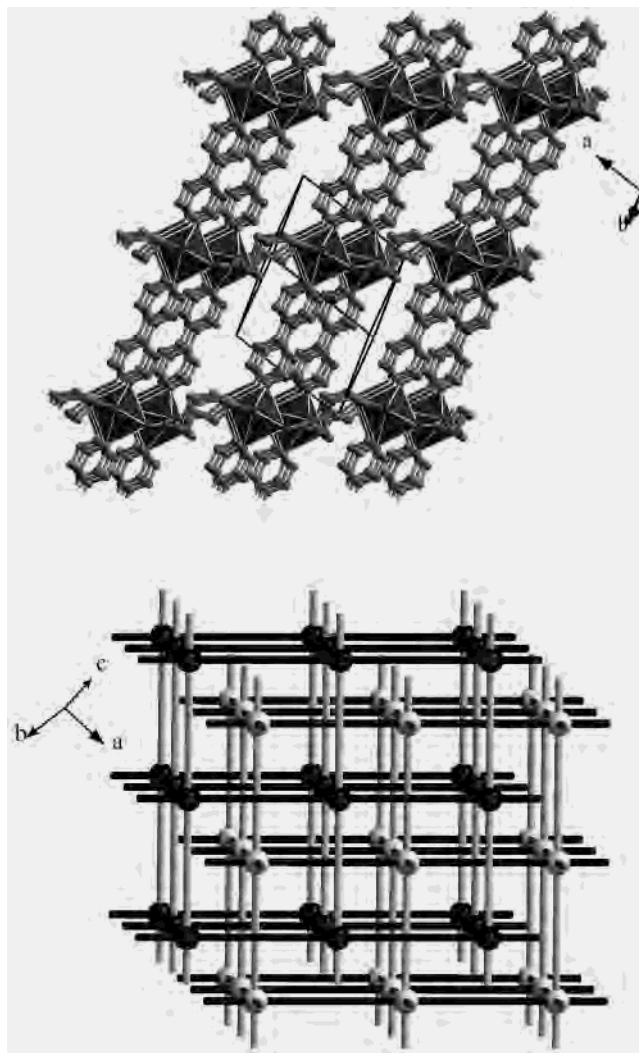
regions 2.088−2.261 Å, and the Mn−N bond distances are 2.280 and 2.295 Å, respectively (Table 4). The flat adipate anions bisbidentately bridge four Mn atoms, and the disordered kinked ones bischelate two Mn atoms, leading to formation of 2D gridlike networks containing 8- and 36-membered rings (ca. 6.5 × 13 Å) (Figure 5). The Mn···Mn separation within the 8-membered ring is 4.035(1) Å larger than the corresponding value in **2**, and the shortest Mn···Mn distance across the bisbidentate adipato group is 10.976-(2) Å, larger than 9.236(2) Å due to the disordered
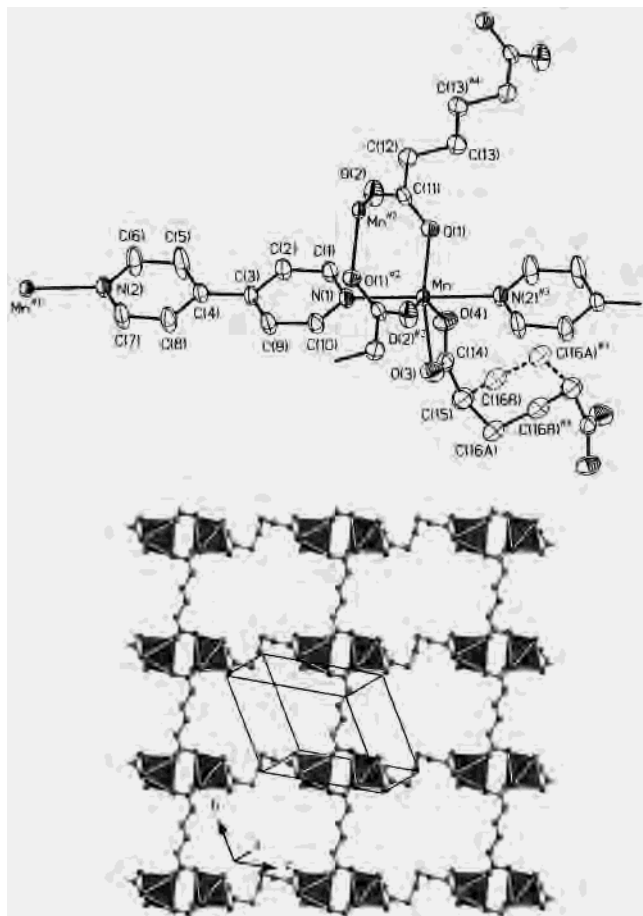
Figure 5. Top: ORTEP view of coordination environments of Mn atoms along with bridging types of adipato and 4,4′-bipyridine ligands and the atomic labeling for **3**. The displacement ellipsoids are drawn at 60% probability level (Symmetry transformations used to generate equivalent atoms: #1 = x, $y - 1$, $z - 1$; #2 = $-x + 1$, $-y + 2$, $-z + 1$; #3 = x, $y + 1$, $z + 1$; #4 = $-x + 2$, $-y + 3$, $-z + 1$; #5 = $-x + 2$, $-y + 2$, $-z + 2$). Bottom: 2D square gridlike network generated from 6-coordinate Mn atoms by bisbidentate and bischelating adipato ligands.


Figure 6. Top: 3D open framework in **3**. Bottom: Topology of the structure of **3** displaying 2-fold interpenetration viewed along the 4,4′-bipyridine ligands (darker and gray rods representing the bischelating and bisbidentate adipato groups, respectively).

bischelating dicarboxylato group. The resulting networks are then pillared by the rigid bpy ligands to generate 3D open framework with the Mn···Mn distance of 11.664(2) Å due to 4,4′-bipyridine ligand. The void spaces in the single framework are so large that two frameworks interpenetrate each other. Figure 6 demonstrates the topology of the structure, which is identical with the well-known Nb_6F_{15} cluster compound containing Nb_6F_{12} clusters made up of niobium centers at the apexes of a regular octahedron with angular μ_2-bridging fluoride ions along the 12 edges of the octahedron.[23] A very recent example of such interpenetration is reported for a zinc terephthalate compound $Zn_8(SiO_4)$-$(C_8H_4O_4)_{12}$, where the bisbidentate terephthalato groups bridge $Zn_8(SiO_4)$ cores into a 3D nanoporous framework.[24]

The above structure description exhibits that the dicarboxylato ligands assume different coordination modes. As far as the *anti*-conformational succinato ligand in **1** is concerned, one end carboxylate group bidentately bridges two Mn atoms in *syn*−*anti* fashion and the other is

monatomically bonded to one Mn atom. Such a bridging fashion of the succinato group is closely similar to that found in $[C_4N_2H_{12}][Cd_2(C_4H_4O_4)_3]\cdot4H_2O$[25] but significantly different from those in $Cd(H_2O)_2(C_4H_4O_4)$[7a] and $Cu(C_4H_4O_4)\cdot$ H_2O.[7b] In the former Cd compound, the gauche succinato group bischelates two metal atoms along with one chelating oxygen atom bonded to the third Cd atom,[7a] while the gauche succinato ligand in the latter chelates one Cu atom through two distal oxygen atoms to form a 7-membered ring with each of the nonchelating oxygen atoms coordinating one Cu atom.[7b] The tridentate glutarato groups in **2** represent a rare example with one terminal carboxylate bidentately bridging two Mn atoms and the other chelating the third Mn atom. To the best of our knowledge, the glutarate anion can function as a monodentate ligand in $[Ni(H_2O)_3(phen)$-$(C_5H_6O_4)]\cdot H_2O$,[26] as a monobidentate bridging ligand in Mn-$(H_2O)_4(C_5H_6O_4)$,[6d] as a bismonodentate bridging ligand in

(23) Schäfer, H.; von Schnering, H. G.; Niehues, K.-J.; Nieder-Vahrenholz, H. G. *J. Less-Common Met.* **1965**, *9*, 95.

(24) Yang, S. Y.; Long, L. S.; Jiang, Y. B.; Huang, R. B.; Zheng, L. S. *Chem. Mater.* **2002**, *14*, 3229.

(25) Vaidhyanathan, R.; Natarajan, S.; Rao, C. N. R. *Inorg. Chem.* **2002**, *41*, 5226.
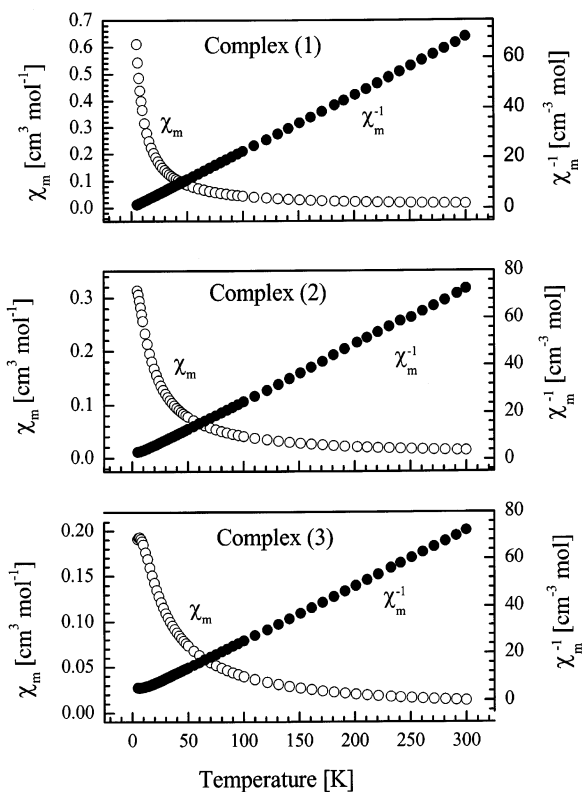
Figure 7. Temperature dependence of the magnetic susceptibilities of **1**−**3** (χ_m being the magnetic susceptibility/Mn(II) ion).

$Mn_2(H_2O)(C_5H_6O_4)$,[10b] as a bischelating ligand in $Cd(H_2O)$-$(C_5H_6O)_4$[27] and as bisbidentate bridging ligands in $[Ag_4-(C_5H_6O_4)]$,[28] $Co(C_5H_6O_4)$,[15a] and $Cu_2(C_5H_6O_4)(bpy)\cdot3H_2O$.[29] In **3**, the two crystallographically distinct adipate anions serve as bischelating and bisbidentate bridging ligands, respectively. The former bischelating fashion of the adipato ligands was reported to be present in $Cd(H_2O)_2(C_6H_8O_4)$,[30] and the latter bisbidentate one was found in $[Eu_2(C_6H_8O_4)_3(H_2O)]\cdot H_2O$.[31] Owing to the different bridging modes, the Mn··· Mn separation over the bidentate carboxylate end in **1** is significantly larger than those in **2** and **3**, respectively. Substitution of the longer adipato ligands for the shorter glutarato ligands is accompanied by the variation of the coordination modes of the dicarboxylate ligands, leading to a transformation of the glutarato-bridged ribbonlike chains in **2** to the adipato-bridged 2D open layers in **3**.

Magnetic Properties

Temperature dependence of the magnetic susceptibility of the title coordination polymers is shown in Figure 7. Compound **1** behaves paramanetically over 5−300 K and obey Curie−Weiss law $\chi_m(T - \Theta) = 4.454(4)$ cm^3 mol^{-1}

with the Weiss constant $\Theta = -1.7(1)$ K. The effective magnetic moment at room temperature is 5.77 μ_B. Slightly different from **1**, the $\chi_m{}^{-1}$ vs T plot for **2** exhibits a considerable deviation upwards from a linearity below 50 K, indicating weak antiferromagnetic behavior at low temperature. Over 50−300 K, the magnetic behavior of **2** follows $\chi_m(T - \Theta) = 4.20(1)$ cm^3 mol^{-1} with the Weiss constant $\Theta = -3.8(4)$ K and the effective magnetic moment at room temperature is 5.75 μ_B. The Neél temperature is below 5 K, which is beyond the lower limit of our measurements. Compound **3** display more significant antiferromagnetic behavior below 55 K with the Neél temperature of 6.9 K. Over 55−300 K, Curie−Weiss law $\chi_m(T - \Theta) = 4.277(6)$ cm^3 mol^{-1} with the Weiss constant $\Theta = -7.2(2)$ K is obeyed and the effective magnetic moment at room temperature is 5.77 μ_B. At room temperature, the three title compounds possess nearly identical effective magnetic moments, which are typical for high-spin manganese(II) compounds.[19] The magnetic measurements suggest that the antiferromagnetic exchange becomes stronger from the succinate through glutarate to adipate compound. Apparently, it is strongly related to the bridging mode of carboxylate groups. The carboxylate groups in **1** interlink Mn atoms in *syn*−*anti* fashion and they bridge Mn atoms in *syn*−*syn* mode in **2** and **3**, indicating the *syn*−*syn* bridging fashion is favorable for antiferromagnetic ordering between Mn atoms.

Conclusion

Under mild ambient conditions, reactions of 4,4′-bipyridine with $Mn(C_4H_4O_4)\cdot4H_2O$ and $Mn(C_5H_6O_4)\cdot4H_2O$ in methanolic aqueous solutions yielded **1** and **2**, respectively, and reaction of freshly prepared $Mn(OH)_{2-2x}(CO_3)_x\cdot yH_2O$, adipic acid, and 4,4′-bipyridine in a methanolic aqueous solution afforded **3**. The title compounds build rare examples of coordination polymers based on cobridging of flexible and rigid spacer ligands. In **1**, tridentate succinato ligands interconnect the 6-coordinate Mn atoms into 2D layers, which are pillared by 4,4-bipyridine ligands into 3D open framework with the free 4,4-bipyridine molecules in cavities. The 6-coordinate Mn atoms in **2** are bridged by glutarate anions into ribbonlike chains, which are further connected by 4,4-bipyridine ligands to generate 2D open layers. Substitution of adipate anions for glutarate anions in **2** resulted in a new coordination polymer **3**, which exhibits 2-fold interpenetration of 3D nanoporous frameworks with the well-known structure type of Nb_5F_{15} cluster compound. Magnetic characterization indicates that the title compounds behave antiferromagnetically at low temperature and the magnetic ordering is strongly related to the bridging fashion of the terminal carboxylate groups of the α,ω-dicarboxylate anions.

(26) Lin, J.-L.; Zheng, Y.-Q.; Kong, Z.-P.; Zhang, H.-L. *Z. Anorg. Allg. Chem.* **2001**, *627*, 1066.
(27) Sun, J.; Zheng, Y.-Q. *Z. Anorg. Allg. Chem.* **2003**, *629*, 1001.
(28) Michailides, A.; Skoulika, S.; Kiritsis, V.; Aubry, A. *J. Chem. Soc., Chem. Commun.* **1995**, 1415.
(29) Rather, B.; Zaworotko, M. J. *Chem. Commun.* **2003**, 830.
(30) Bakalbassis, E. G.; Korabik, M.; Michailides, A.; Mrozinski, J.; Raptopoulou, C.; Skoulika, S.; Terzis, A.; Tsaousis, *D. J. Chem. Soc., Dalton Trans.* **2001**, 850.
(31) Kim, Y. J.; Suh, M.; Jung, D.-Y. *Inorg. Chem.* **2003**, *42*, in press.